Dynamic Analysis of Electrostatic MEMS by Meshless Methods

Gang Li and N. R. Aluru

Beckman Institute for Advanced Science and Technology
University of Illinois at Urbana-Champaign
405 N. Mathews Avenue, Urbana, IL 61801

ABSTRACT

Electrostatically actuated microstructures are widely used in microelectromechanical systems (MEMS). Computational analysis of electrostatic MEMS requires a self-consistent solution of the interior elastic domain and the exterior electrostatic domain. This paper proposes an efficient approach to carry out the dynamic analysis of electrostatic MEMS structures. The approach employs a meshless Finite Cloud Method (FCM) to solve the interior mechanical domain of the structures and a scattered point Boundary Cloud Method (BCM) to solve the exterior electrostatic domain. Lagrangian descriptions are used in both mechanical and electrostatic analyses. The electrostatic forces and mechanical deformations are all computed on the undeformed configuration of the structures. The approach provides an efficient computational tool for dynamic analysis of electrostatic MEM devices.

Keywords: coupled electro-mechanical analysis, meshless, finite cloud method, boundary cloud method, Lagrangian description

1 INTRODUCTION

Computational analysis of electrostatic MEMS requires a self-consistent solution of the coupled interior mechanical domain and the exterior electrostatic domain [1]. Conventional methods for coupled domain analysis, such as FEM/BEM, require mesh generation, mesh compatibility, re-meshing and interpolation of solution between the domains. Mesh generation can be difficult and time consuming for complex geometries. Furthermore, mesh distortion can occur for micromechanical structures that undergo large deformations. To overcome all these difficulties, we propose an efficient approach to perform static and dynamic analysis of electrostatically actuated MEMS.

The primary contributions of the paper are as follows: (1) Our approach employs a meshless Finite Cloud Method (FCM)[2,3] to solve the interior structural domain. The Finite Cloud Method is a true meshless method in which only points are needed to cover the structural domain and no connectivity information among the points is required. This method completely eliminates the meshing process and radically simplifies the analysis procedure. (2) A Boundary Cloud Method (BCM) [4] is used to analyze the exterior electrostatic domain to compute the electrostatic forces acting on the surface of the structures. The BCM utilizes a meshless interpolation technique and a cell based integration. Besides the flexibility of the cell integration, the BCM is an excellent match to the FCM for coupled domain analysis since both of them have meshless interpolations. (3) A Lagrangian description [5] of the boundary integral equation is developed and implemented with BCM. Typically, the mechanical analysis is performed by a Lagrangian approach using the undeformed position of the structures. However, the electrostatic analysis is performed by using the deformed position of the conductors. The Lagrangian description maps the electrostatic analysis to the undeformed position of the conductors. Thus, the electrostatic forces and mechanical deformations are all computed on the undeformed configuration of the structures. The Lagrangian description eliminates the requirement of geometry updates and recomputation of the interpolation functions.

2 ELECTRO-MECHANICAL ANALYSIS

Electrostatically actuated microstructures can undergo large deformations for certain geometric configurations and applied voltages. In this paper, we perform 2-D geometrically nonlinear analysis of microstructures. For electro-mechanical analysis, the transient governing equations for an elastic body using a Lagrangian description are given by [6]

$$\rho_0 \ddot{\mathbf{u}} = \nabla \cdot (\mathbf{FS}) \qquad in \quad \Omega \qquad (1)$$
$$\mathbf{u} = \mathbf{G} \qquad in \quad \Gamma_g \qquad (2)$$
$$\mathbf{P} \cdot \mathbf{N} = \mathbf{H} \qquad in \quad \Gamma_h \qquad (3)$$
$$\mathbf{u}|_{t=0} = \mathbf{G_0} \qquad in \quad \Omega \qquad (4)$$
$$\dot{\mathbf{u}}|_{t=0} = \mathbf{V_0} \qquad in \quad \Omega \qquad (5)$$

where $\mathbf{F}$ is the deformation gradient, $\mathbf{u}$, $\dot{\mathbf{u}}$ and $\ddot{\mathbf{u}}$ are the displacement, velocity and acceleration vectors, respectively, $\mathbf{N}$ is the unit outward normal vector in the initial configuration, $\mathbf{S}$ is the second Piola-Kirchhoff stress, $\mathbf{G}$ is the prescribed displacement, $\mathbf{G_0}$ and $\mathbf{V_0}$ are the initial displacement and velocity, respectively, $\mathbf{H}$ is the electrostatic pressure acting on the surface of the structures and $\mathbf{P}$ is the first Piola-Kirchhoff stress tensor.

A Newmark scheme with an implicit trapezoidal rule is used for solving the dynamic problem of the nonlinear elastic domain. The flow chart for dynamic electro-mechanical analysis is shown in Figure 1.

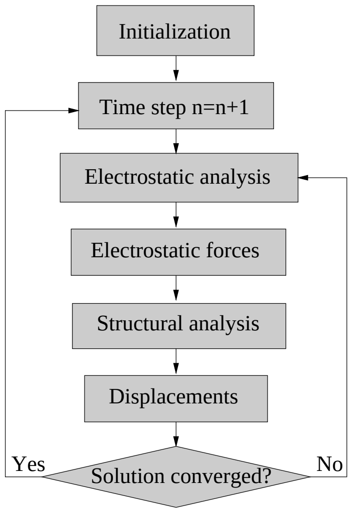

Figure 1: Flow chart for the dynamic electro-mechanical analysis.

3 FCM FOR MECHANICAL ANALYSIS

The meshless Finite Cloud Method (FCM) [2,3] uses a fixed kernel approximation to construct the interpolation functions and a point collocation technique to discretize the governing partial differential equations. In a 2-D fixed kernel approach, an approximation $u^a(x,y)$ to an unknown $u(x,y)$ is given by

$$u^a(x,y) = \int_\Omega C(x,y,x_k-s,y_k-t)\phi(x_k-s,y_k-t)u(s,t)dsdt \tag{6}$$

where $C(x,y,x_k-s,y_k-t)$ is the correction function which is given by

$$C(x,y,x_k-s,y_k-t) = \mathbf{P}^T(x_k-s,y_k-t)\mathbf{C}(x,y) \tag{7}$$

ϕ is the kernel function which is usually taken as a cubic spline or a Gaussian function and $\mathbf{P}^T = \{p_1, p_2, \ldots, p_m\}$ is an $m \times 1$ vector of basis functions. In this paper, 2-D quadratic basis $\mathbf{P}^T(x,y) = [1, x, y, x^2, xy, y^2]$ is used. $\mathbf{C}(x,y)$ are the unknown correction function coefficients computed by satisfying the consistency conditions (see [2,3] for details). The discrete form of the approximation $u^a(x,y)$ is given by

$$u^a(x,y) = \sum_{I=1}^{NP} N_I(x,y)\hat{u}_I \tag{8}$$

where $\hat{u}_I$ is the nodal parameter for node I, and $N_I(x,y)$ is the fixed kernel interpolation function (see [2,3] for details). The derivatives of the unknown u are approximated by

$$\frac{\partial u^a(x,y)}{\partial x} = \sum_{I=1}^{NP} \frac{\partial N_I(x,y)}{\partial x}\hat{u}_I \tag{9}$$

$$\frac{\partial^2 u^a(x,y)}{\partial x^2} = \sum_{I=1}^{NP} \frac{\partial^2 N_I(x,y)}{\partial x^2}\hat{u}_I \tag{10}$$

In electro-mechanical analysis, the displacements u and v and their derivatives are approximated by using Eq. (8-10). Substituting the approximations into Eq. (1), one gets a non-linear system of equations

$$f_j(\hat{u}_1, \hat{u}_2, \ldots, \hat{u}_{NP}; \hat{v}_1, \hat{v}_2, \ldots, \hat{v}_{NP}) = 0 \quad j = 1,2 \tag{11}$$

The resultant non-linear system is solved by using a Newton's method. Boundary conditions are enforced on the boundary points where Dirichlet or Neumann boundary conditions are specified. The governing equations for such boundary points are replaced by the corresponding boundary conditions.

4 LAGRANGIAN ELECTROSTATICS

When electrostatic potentials are applied on microstructures, electrostatic forces are generated on the surfaces of the microstructures. The surface charge density on the structure needs to be computed to obtain the electrostatic forces. The 2D governing equation for electrostatic analysis can be written in a boundary integral form as [7]

$$\phi(p) = \int_{d\omega} \frac{1}{\epsilon} G(p,q)\sigma(q)d\gamma_q + C \tag{12}$$

$$\int_{d\Omega} \sigma(q)d\gamma_q = C_T \tag{13}$$

where ϵ is the dielectric constant of the medium, p is the source point, q is the field point which moves along the boundary of the conductors and G is the Green's function. In two dimensions, $G(p,q) = ln|p-q|/2\pi$, where $|p-q|$ is the distance between the source point p and the field point q. C_T is the total charge of the system and C is an unknown variable which can be used to compute the potential at infinity.

Equations (12) and (13) are defined in the deformed configuration of the conductors, i.e., the surface charge density is computed by solving the boundary integral equations on the deformed geometry of the conductors.

We refer to this approach as the deformed configuration approach. The need to update the geometry of the structures in the deformed configuration approach presents several difficulties (see [5] for details). In this paper, we employ a Lagrangian approach [5] to compute the surface charge density in the undeformed configuration of the conductors. In the Lagrangian approach, the boundary integral equations, Eq.(12-13), can be rewritten as

$$\phi(p(P)) = \int_{d\Omega} \frac{1}{\epsilon} G(p(P), q(Q)) \sigma(q(Q)) \left[\mathbf{T}(Q) \cdot \mathbf{C}(Q)\mathbf{T}(Q)\right]^{\frac{1}{2}} d\Gamma_Q + C \qquad (14)$$

$$\int_{d\Omega} \sigma(q(Q)) \left[\mathbf{T}(Q) \cdot \mathbf{C}(Q)\mathbf{T}(Q)\right]^{\frac{1}{2}} d\Gamma_Q = C_T \qquad (15)$$

where P and Q are the source and field points in the initial configuration corresponding to the source and field points p and q in the deformed configuration, $\mathbf{T}(Q)$ is the tangential unit vector at field point Q and $\mathbf{C}(Q)$ is the Green deformation tensor.

5 BCM FOR ELECTROSTATIC ANALYSIS

In this paper, we employ a boundary cloud method to solve the Lagrangian description of the electrostatic governing equations (Eq.(14-15)). In a boundary cloud method, the surface of the domain is discretized into scattered points. The points can be sprinkled randomly covering the boundary of the domain. Interpolation functions are constructed by centering a weighting function at each point or node. For the electro-mechanical problem, the potential ϕ is prescribed on the structures. The unknown surface charge density σ in the vicinity of the point t is approximated by a truncated Hermite-type interpolation[4]

$$\sigma(x, y) = \mathbf{p}^T(x, y)\mathbf{a}_t \qquad (16)$$

where $\mathbf{p}$ is the base interpolating polynomial (see section 3) and $\mathbf{a}_t$ is the unknown coefficient vector for point t. For a point t, the unknown coefficient vector $\mathbf{a}_t$ is computed by using a least-squares approach (see [4] for details). The discrete form of the truncated Hermite approximation for the unknowns is given by

$$\sigma(x, y) = \sum_{I=1}^{NP} \overline{M}_I(x, y)\tilde{\sigma}_I \qquad (17)$$

The boundary of the structure is discretized into cells for integration purpose. Each cell contains a certain number of nodes and the number of nodes can vary from cell to cell. Different from an element or a panel in boundary-element methods, the cell can be of any shape or size and the only restriction is that the union of all the cells equal the boundary of the domain. Assuming that the boundary is discretized into NC cells and substituting the truncated Hermite-type approximation for the unknown charge density, the boundary integral equation for the electrostatic problem given in Eq. (14-15) can be rewritten in a matrix form as

$$\mathbf{M}\tilde{\sigma} = \overline{\phi} \qquad (18)$$

where $\mathbf{M}$ is an $(NC{+}1)\times(NC{+}1)$ coefficient matrix and $\overline{\phi}$ and $\tilde{\sigma}$ are $(NC+1)\times 1$ right hand side and unknown vector, respectively. By substituting the potential on the conductors and the total charge into Eq. (18), the surface charge density can be computed from Eq. (17) and Eq. (18).

6 NUMERICAL RESULTS

The first example is the static analysis of a micromirror structure. Figure 2 shows the surface charge density on the electrodes when a potential of 40 volts is applied. The peak rotation of the mirror structure as a function of the applied voltage is shown in Figure 3.

In the second example, dynamic behavior of a cantilever beam and a fixed-fixed beam is analyzed. The geometry of the cantilever and fixed-fixed beams is: $80\mu m$ long, $0.5\mu m$ thick and $10\mu m$ wide. The gap is $0.7\mu m$. The Young's modulus of the beams is 169 GPa, the density of the beams is 2331 kg/m^3 and the Poisson ratio is 0.3. In the cantilever beam case, the pull-in voltage is 2.40V from the quasi-static analysis (Figure 4) and is 2.18V in the dynamic analysis (Figure 5). The difference is about 9%. In the fixed-fixed beam case, the pull-in voltage is 18.0V from the quasi-static analysis (Figure 6) and 16.4V from the dynamic analysis (Figure 7). The difference is again about 9%. For a bias of 2.18V, the transient deflection of the tip of the cantilever beam is shown in Figure 5. A time step of 0.1 μs is employed. For a bias of 16.4V, the transient deflection of the center of the fixed-fixed beam is shown in Figure 7. A time step of 0.04 μs is employed.

7 CONCLUSIONS

In summary, this paper presents a new numerical approach to perform coupled electromechanical analysis. The approach radically simplifies the coupled domain analysis as mesh generation of complex micromechanical structures is eliminated.

REFERENCES

[1] N. R. Aluru and J. White, "An Efficient Numerical Technique for Electromechanical Simulation of Complicated Microelectromechanical Structures", Sensors and Actuators A, 58, 1-11, 1997.

[2] N. Aluru and Gang Li, "Finite Cloud Method: A True Meshless Technique Based On A Fixed Reproducing Kernel Approximation", International Journal for Numerical Methods in Engineering, 50(10), 2373-2410, 2001.

[3] Xiaozhong Jin, Gang Li and N. R. Aluru, "On the Equivalence Between Least-Squares and Kernel Approximation in Meshless Methods", Computer Modeling in Engineering and Sciences, 2(4), 447-462, 2001.

[4] Gang Li and N. R. Aluru, "Boundary Cloud Method: A Combined Scattered Point/Boundary Integral Approach for Boundary-Only Analysis", Accepted for publication in Computer Methods in Applied Mechanics and Engineering, 2001.

[5] Gang Li and N. R. Aluru, "A Lagrangian approach to compute electrostatic forces on deformable MEMS", Accepted for publication in Journal of MEMS, 2001.

[6] D. S. Chandrasekharaiah and L. Debnath, Continuum Mechanics, Academic Press, 1994.

[7] F. Shi, P. Ramesh and S. Mukherjee, "On the Application of 2D Potential Theory to Electrostatic Simulation", Communications in Numerical Methods in Engineering, 11, 691-701, 1995.

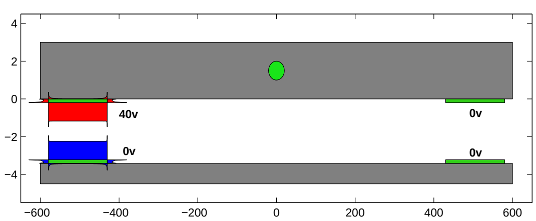

Figure 2: Electrostatic micro-mirror structure.

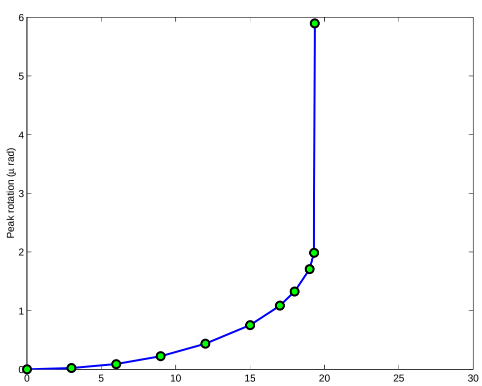

Figure 3: Pull-in analysis of electrostatic micro-mirror.

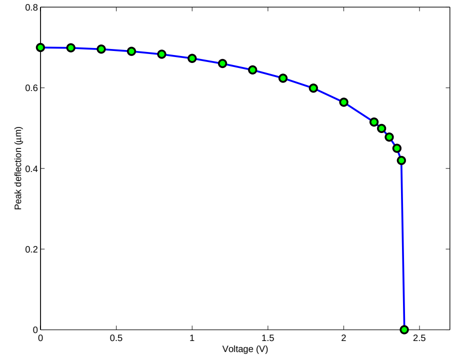

Figure 4: Static pull-in analysis of a Cantilever switch.

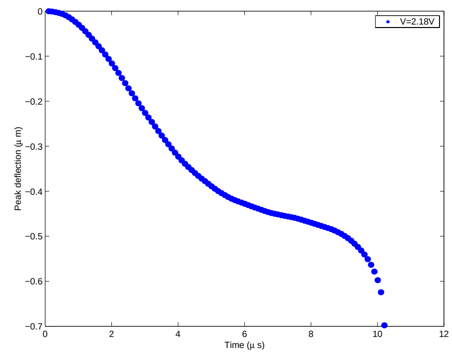

Figure 5: Dynamic pull-in analysis of a Cantilever switch.

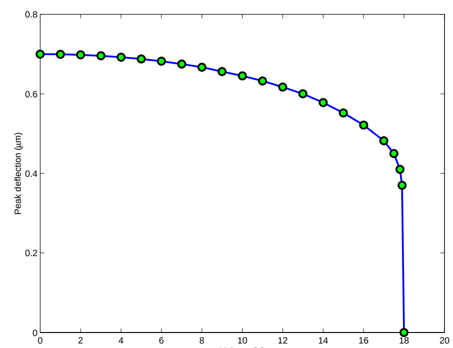

Figure 6: Static pull-in analysis of a Fixed-fixed switch.

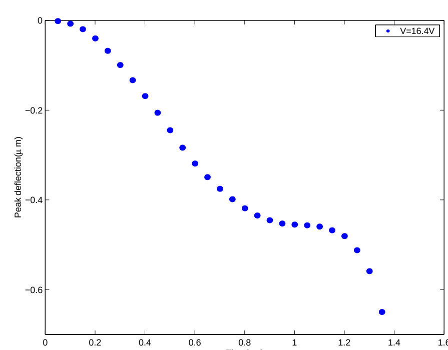

Figure 7: Dynamic pull-in analysis of a Fixed-fixed switch.